

Further Analysis of the Period-Three Route to Chaos in Passive Dynamic Walking of a Compass-Gait Biped Robot

Hassène Gritli

Direction Générale des Etudes Technologiques
Institut Supérieur des Etudes
Technologiques de Kélibia
8090 Kélibia, Tunisia
Email: grhass@yahoo.fr

Nahla Khraief

Université de Carthage
Ecole Supérieure de Technologie
et d'Informatique
2035 Charguia II, Tunis, Tunisia
Email: nahla_khraief@yahoo.fr

Safya Belghith

Université de Tunis El Manar
Ecole Nationale d'Ingénieurs
de Tunis
1002 Tunis, Tunisia
Email: safya.belghith@enit.rnu.tn

Abstract—This paper continues our investigations into the period-three route to chaos exhibited in the passive dynamic walking of a compass-gait biped robot [8]. The further analysis on the resulting chaos is made by Lyapunov exponents and fractal dimension. The chaotic attractor, its first return and its basin of attraction are presented. In addition, the study of the period-3 passive gait is also performed. The balance between potential and kinetic energies has been illustrated. Furthermore, the limit cycle in phase space, the temporal evolution and the basin of attraction of this period-three gait were also presented in the paper.

I. INTRODUCTION

One of the most interesting applications of robotics is the analysis of human walking through various prototypes bipeds. Studies were found to solve some problems related to the stability of human walking and also in relation to the design of active and passive prostheses of lower human members. However, despite its simplicity, human walking is considered as a very complex dynamic system and it is not well understood. Dynamic walking biped robots is modeled by an impulsive hybrid nonlinear dynamics. In order to obtain a synergy between human walking gaits and study of biped robots, a two-link biped mechanism will be a good experimental/theoretical base model.

In the concept of bipedal robotics, passive dynamic walking has attracted the attention of many researchers and has been considered as the starting point for the control of biped robots. Passive dynamic walking is a form of bipedal locomotion for which a biped robot requires no exogenous source of energy, but it uses gravity to walk on an inclined plane. This walking mode solves the problem of energy consumption of bipedal robots and achieve maximum energy efficiency. In addition, the use of passive dynamics should also get additional insights into the design principles of pedestrian locomotion in nature. The best-known biped robot using the passive dynamic walking is the compass-gait biped robot. This biped is a two link mechanism that was originally designed in 1996 by Goswami *et al.* [1], [2]. These researchers have shown that this type of bipedal walking can generate chaos and period doubling bifurcations. Until today, many researchers are working on passive dynamic walking of the compass biped robot and other simple biped robots to find other properties that can help in the

understanding of human walking. Thus, chaos on the passive dynamic walking of biped robots has been studied and several properties of the chaotic gaits are noticed. Authors in [10], [11] investigated chaos in the passive walking model of a point-foot walker.

We have recently shown that a cyclic-fold bifurcation is generated in the passive dynamic walking of the compass-gait biped. This bifurcation gives rise to a cascade of period-doubling bifurcations and a resulting route to chaos [8]. This bifurcation creates a pair of a period-3 stable gait and a period-3 unstable gait. In addition, we have shown that the passive gait of a biped robot with unequal leg length displays also the cyclic-fold bifurcation with a hysteresis [4]. In addition, we have shown in [6] that this walking locomotion has two additional routes to chaos namely the intermittency route and the interior-crisis route. We also showed in [5], [7] that the compass-gait biped robot falls because of the emergence of a global bifurcation known as the boundary crisis. This type of global bifurcation is generated mainly through the unstable period-3 limit cycle. In [3], we used an energy-tracking controller to stabilize and follow the period-3 passive dynamic walking of the compass biped robot. In [9], we controlled chaos exhibited in passive dynamic walking of the compass-gait biped robot to obtain a period-1 stable gait.

In this paper, we will analysis the passive dynamic walking of the compass-gait biped robot. We will give more results on the period-three passive limit cycle and the corresponding route to chaos. Our analysis focuses first on the calculation of Lyapunov exponents and fractal dimension to quantify order and chaos. We will present different attractive structures of the chaotic attractor. The Poincaré first return map of the chaotic attractor and its basin of attraction are also presented. Moreover, we study the period-three passive limit cycle in the bi-dimensional phase space, the time evolution of different state variables, and the balance of kinetic and potential energies. We also study the basin of attraction of the period-three passive gait compared to the basin of attraction of the period-one passive gait.

II. PASSIVE DYNAMIC WALKING OF THE COMPASS-GAIT BIPED ROBOT

A. The Compass-Gait Biped Robot

Fig. 1 provides an illustrative representation of the compass-gait biped robot where the important parameters in the dynamics description are given in Table I [2], [8]. Such biped robot is a subclass of rigid mechanical systems subject to unilateral constraints. The compass-gait biped robot is composed of a stance leg and a swing leg. The two legs are modeled as rigid bars without knees and feet, and with a frictionless hip. For adequate initial conditions and a corresponding slope angle φ , the compass-gait biped robot performs a passive walk without any external intervention. However, it is powered only by gravity. The passive walking dynamics of the compass-gait biped robot is limited in the sagittal plane and is mainly composed of two phases: an oscillation (swing) phase and an impact phase. In the first case, the biped is modeled as a double pendulum. The latter case occurs when the swing leg strikes the ground and the stance leg leaves the ground. In Fig. 1, θ_s is the support angle, whereas θ_{ns} is the nonsupport (swing) angle.

B. Impulsive Hybrid Non-Linear Dynamics

It is well known up to now that the dynamic model of the passive walking of the compass-gait biped robot consists of nonlinear differential equations for the swing phase and algebraic equations for the impact phase [8].

1) *Continuous Dynamics of the Swing Phase:* Let $\theta = [\theta_{ns} \ \theta_s]^T$ be the vector of generalized coordinates of the compass-gait biped robot. The motion of the compass-gait

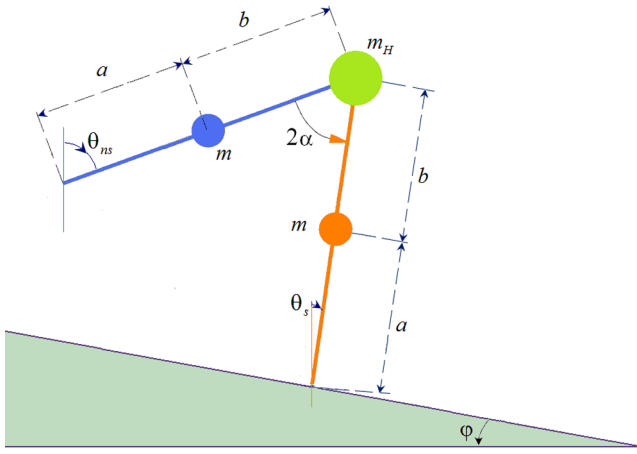


Fig. 1. The compass-gait biped robot down a walking surface of slope φ .

TABLE I. PARAMETERS SPECIFICATION OF THE COMPASS-GAIT BIPED MODEL

Symbol	Description	Value
a	Lower leg segment	0.5 m
b	Upper leg segment	0.5 m
m	Mass of leg	5 kg
m_H	Mass of hip	10 kg
g	Gravitational constant	9.8 m/s ²

biped robot is described by the following Lagrangian system :

$$\mathcal{J}(\theta)\ddot{\theta} + \mathcal{H}(\theta, \dot{\theta}) + \mathcal{G}(\theta) = \mathbf{0} \quad (1)$$

This continuous dynamics is indeed subject to the following natural unilateral constraints:

$$\Omega = \{\theta \in \mathbb{R}^2 : \Phi(\theta) = l(\cos(\theta_s + \varphi) - \cos(\theta_{ns} + \varphi)) > 0\} \quad (2)$$

with $l = a + b$.

Matrices in (1) are defined by:

$$\begin{aligned} \mathcal{J}(\theta) &= \begin{bmatrix} mb^2 & -mlb\cos(\theta_s - \theta_{ns}) \\ -mlb\cos(\theta_s - \theta_{ns}) & m_H l^2 + m(l^2 + a^2) \end{bmatrix}, \\ \mathcal{H}(\theta, \dot{\theta}) &= \begin{bmatrix} mlb\dot{\theta}_s^2 \sin(\theta_s - \theta_{ns}) \\ -mlb\dot{\theta}_{ns}^2 \sin(\theta_s - \theta_{ns}) \end{bmatrix}, \\ \mathcal{G}(\theta) &= g \begin{bmatrix} mbsin(\theta_{ns}) \\ -(m_H l + m(a + l))\sin(\theta_s) \end{bmatrix}. \end{aligned}$$

2) *Algebraic Equations of the Impact Phase:* Algebraic equations of the impact phase are given by:

$$\begin{cases} \theta^+ = \mathcal{R}_e \theta^- \\ \dot{\theta}^+ = \mathcal{S}_e \dot{\theta}^- \end{cases} \quad (3)$$

where subscribes $^+$ and $^-$ denotes just after and just before the impact phase, respectively.

Matrices in (3) are defined by: $\mathcal{R}_e = \begin{bmatrix} 0 & 1 \\ 1 & 0 \end{bmatrix}$,

$\mathcal{S}_e = \mathcal{Q}_p^{-1}(\theta) \mathcal{Q}_m(\theta)$, with

$$\mathcal{Q}_m(\theta) = \begin{bmatrix} -mab & -mab + (m_H l^2 + 2mal)\cos(2\alpha) \\ 0 & -mab \end{bmatrix},$$

and

$$\mathcal{Q}_p(\theta) = \begin{bmatrix} mb^2 - \mu & l^2(m_H + m) + ma^2 - \mu \\ mb^2 & -\mu \end{bmatrix}, \text{ where } \mu = mbl\cos(2\alpha) \text{ and } \alpha = \frac{1}{2}(\theta_s - \theta_{ns}) \text{ is the half-interleg angle (see Fig. 1).}$$

The impact phase occurs when:

$$\begin{cases} \Phi_1(\theta) = l(\cos(\theta_s + \varphi) - \cos(\theta_{ns} + \varphi)) = 0 \\ \Phi_2(\theta, \dot{\theta}) = \frac{\partial \Phi_1(\theta)}{\partial \theta} \dot{\theta} < 0 \end{cases} \quad (4)$$

C. Passive Walking Patterns of the Compass Biped

The bifurcation diagram of Fig. 2a offers all passive gaits of the compass biped robot [7], [8], [9]. Here, the bifurcation parameter is the angle of the slope φ . In this bifurcation diagram, the blue attractor A_1 is the classic behavior exhibited by the compass-gait biped robot: a cascade of period-doubling bifurcations leading to chaos. However, the pink attractor A_2 is that recently found by us in [8]. This attractor reveals a scenario of period-3 route to chaos. Fig. 2b shows clearly this route. The attractor A_2 was born by the cyclic-fold bifurcation (marked as CFB). This bifurcation occurs at $\varphi = 3.8734$ deg. At this bifurcation, a period-three stable periodic orbit (p3-SPO) collides with a period-3 unstable periodic orbit (p3-UPO). This p-3 UPO is responsible for generating a double boundary crisis (marked as BC), which is the main cause of the fall of the compass-gait biped robot [7]. For the conventional attractor A_1 , the route of period-doubling to chaos is born from a period-1 stable gait (p1-SPO). Chaos is terminated by the boundary crisis at $\varphi = 5.201$ deg. However, in Fig. 2b, the period-three stable gait exhibits a period-doubling leading

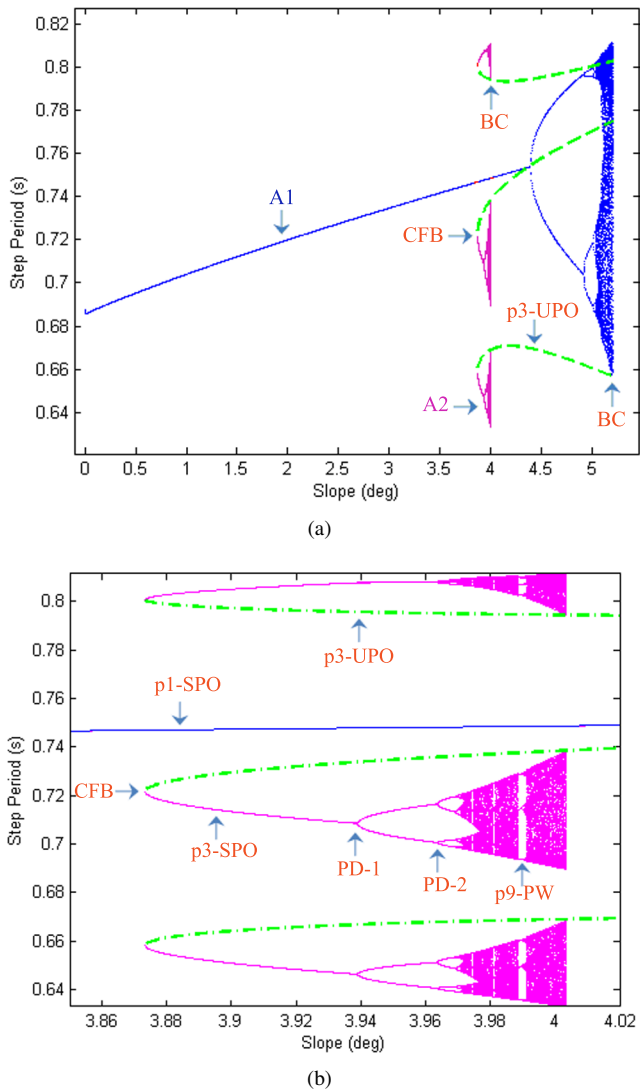


Fig. 2. Bifurcation diagrams: step period as a function of the slope angle φ . (b) is an enlargement of (a).

to the formation of chaos. Chaos is found to be dead at $\varphi = 4.0036$ deg. Some periodicity windows (PW) appeared. The window that is marked by p9-PW in Fig. 2b reveals a scenario of period-doubling route to chaos from a period-9 passive gait [8].

III. ANALYSIS OF THE PERIOD-THREE ROUTE TO CHAOS

A. Investigation of Order/Chaos via Lyapunov Exponents and Fractal Dimension

Since the passive dynamics of the compass-gait biped robot is four-dimensional, then we have four Lyapunov exponents. Variation of the spectrum of the Lyapunov exponents and the fractal Lyapunov dimension with respect to the slope angle φ are given by Fig. 3a and Fig. 3b, respectively. Fig. 4 presents the two largest Lyapunov exponents λ_1 and λ_2 . These diagrams are depicted for slopes between 3.85 deg and 4.02 deg. Recall that the cyclic-fold bifurcation is born at $\varphi = 3.8734$ deg, and chaos of the attractor A_2 is terminated at $\varphi = 4.0036$ deg. The phenomenon of period-three route to chaos occurs between

3.8734 deg and 4.0035 deg. Outside of this range, the passive walking pattern is of period-1 (marked as p1-SPO). Obviously, in this range, the first (largest) Lyapunov exponent λ_1 is zero while the three remaining Lyapunov exponents are negative for slopes between 3.8734 deg and 3.9708 deg. In this interval of slopes, the passive gait of the compass biped robot is periodic and it exhibits a cascade of period-doubling bifurcations when the slope angle increases. The period-doubling (PD) phenomenon is expressed in each diagram with a cascade of parabolic curves. Furthermore, the attractor dimension remains almost constant at an integer value 1 when the gait is periodic except at the period-doubling bifurcations where the Lyapunov dimension is equal to 2.

However, for slopes higher than 3.9708, the largest Lyapunov exponent, λ_1 (λ_2), oscillates between positive (zero) and zero (negative) values corresponding to chaotic and periodic gaits. The two other Lyapunov exponents, λ_3 and λ_4 , remain always negative. The periodic gaits bring in fact about the existence of periodicity windows in the chaotic regime. In addition, we emphasize that λ_1 reaches its highest value which is equal to 0.3 at $\varphi = 4.0035$ deg. Moreover, when the passive walking pattern is chaotic, the Lyapunov dimension is found to be higher than 2 and increases to reach its maximum fractal value 2.15 at $\varphi = 4.0035$ deg.

B. Investigation of the Chaotic Attractor

1) *The Chaotic Attractor and its First Return Map*: Fig. 5 shows different forms of the chaotic attractor in different phase-spaces for the slope angle $\varphi = 4.0035$ deg. The passive dynamic walking is described by a complete disappearance of order and is an extreme case of an asymmetric gait and affirming thus that the attractor is chaotic.

Obviously, in Fig. 5b and Fig. 5c, the form of the chaotic attractor is quite attractive. Fig. 5b shows the chaotic attractor in 2D plotted with respect to the angular velocities of the two legs of the compass-gait biped robot. The chaotic attractor seems like a butterfly. In addition, Fig. 5c manifests another structure of the chaotic attractor plotted in the three-dimensional state-space. The chaotic attractor has the shape of a heart. The largest Lyapunov exponent and the fractal dimension were computed to be about 0.3 and 2.15, respectively.

Fig. 6 shows the Poincaré first return map in 2D. Fig. 6b is an enlargement of Fig. 6a. The first return map is composed of an infinite number of points irregularly distributed in three curved arcs. By expanding the right part (Fig. 6b), we note that the Poincaré first return map consists of several closed lines separated by empty spaces. This confirms that the attractor is chaotic and it has a fractal dimension.

2) *Basin of Attraction of the Chaotic Attractor*: Fig. 7 shows the basin of attraction of the chaotic gait and that of the period-one gait. The pink set is the basin of attraction of the chaotic attractor. However, the blue set reveals the basin of attraction of the period-one gait. Here, the basin of attraction is plotted for a fixed initial position of the two legs. We have chosen $\theta_{ns} = -21$ deg, and θ_s such that $\theta_s + \theta_{ns} + 2\varphi = 0$. It is obvious that the basin of attraction of the chaotic attractor is smaller than that of the period-one passive gait. Thus, a small perturbation on the initial conditions of the compass biped robot can bring the behavior of the period-one passive walk

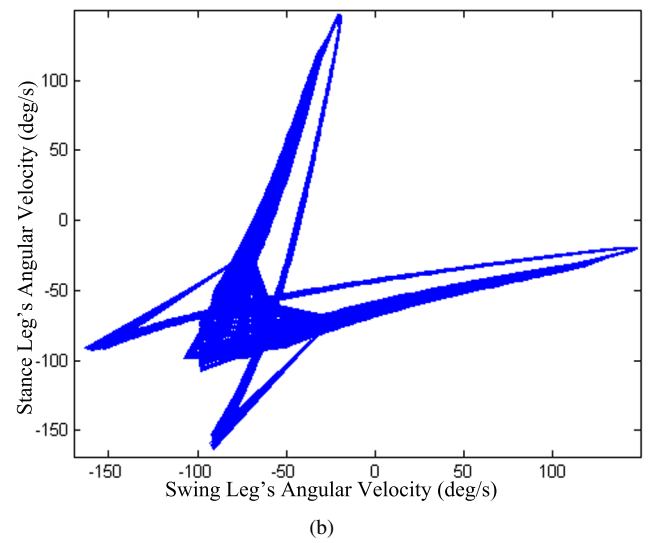
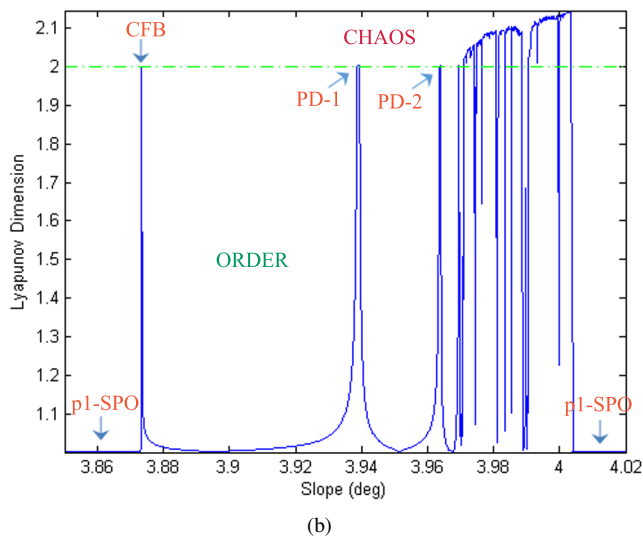
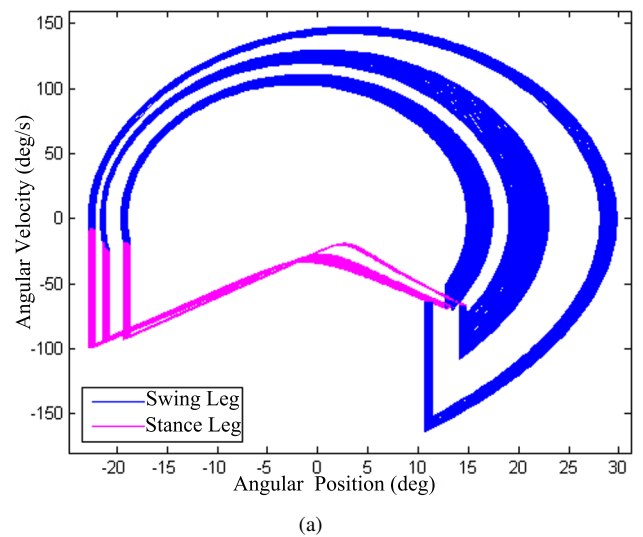
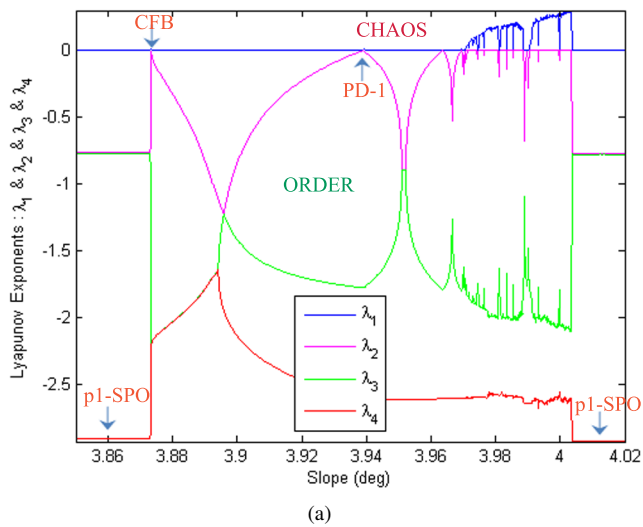


Fig. 3. Variation of Lyapunov exponents (a) and Lyapunov dimension (b) as ϕ .

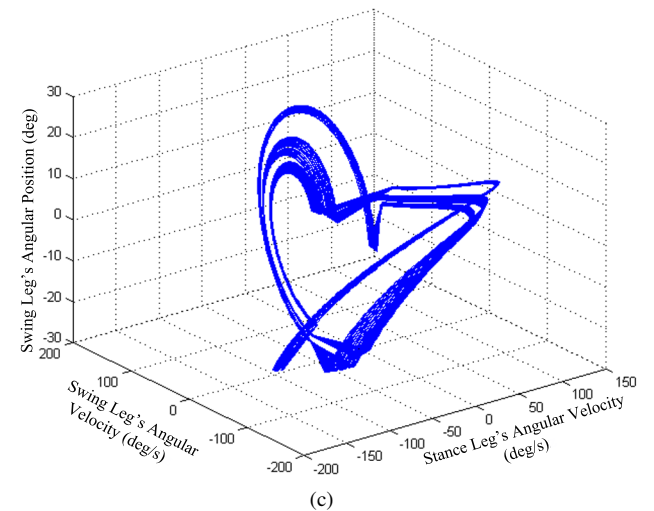
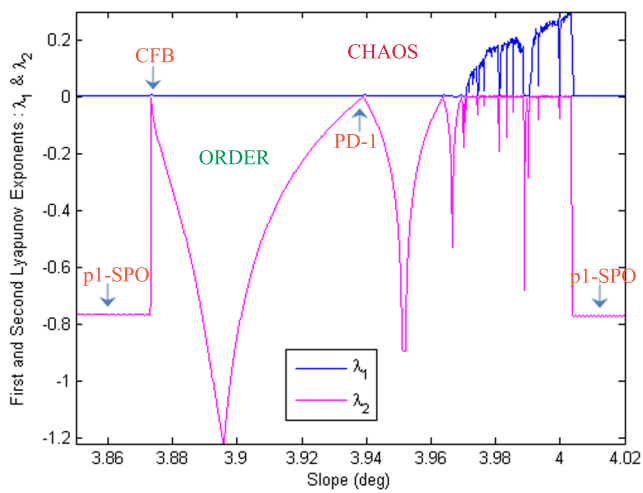


Fig. 5. Chaotic attractor for $\phi = 4.0035$ deg in different state-spaces.

Fig. 4. Variation of the two largest Lyapunov exponents λ_1 and λ_2 . This is an enlargement of Fig. 3a.

to another completely different form of locomotion, i.e. the chaotic gait.

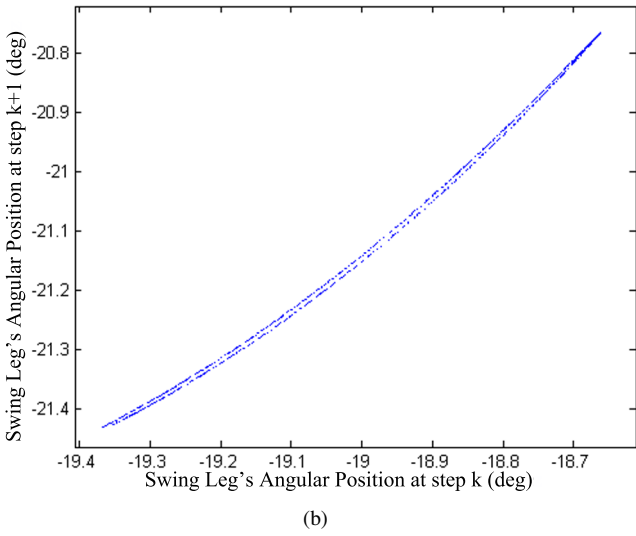
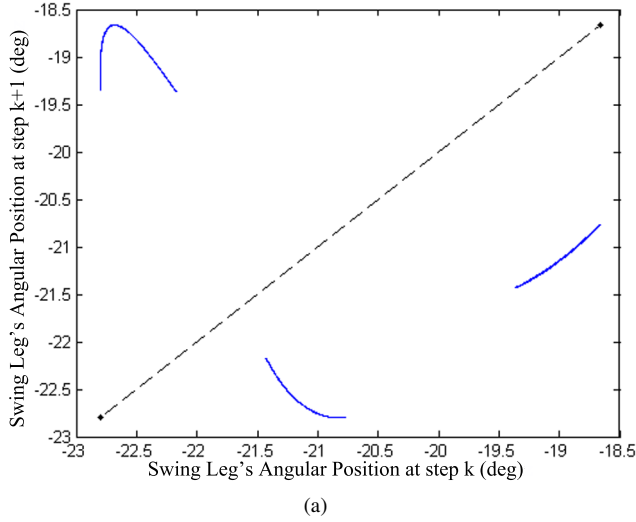


Fig. 6. First return map for $\varphi = 4.0035$ deg. (b) is an enlargement of (a).

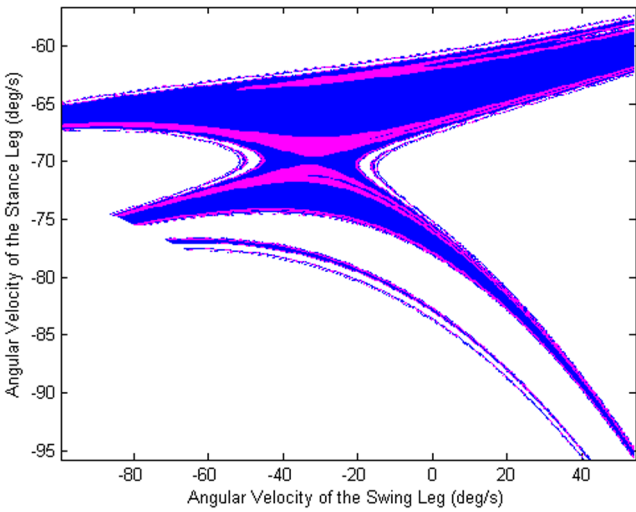


Fig. 7. Basin of attraction of the chaotic attractor compared with that of the period-one limit cycle for the same slope $\varphi = 4.0035$ deg.

C. Analyze of the Period-Three Gait

In this subsection, we focus on the analyze of the period-three passive gait of the compass biped robot. Then, we choose the slope angle $\varphi = 3.92$ deg.

1) *Period-Three Gait in the Phase-Plane:* Fig. 8 shows the angular velocity of each leg as a function of its angular position. In this state-space, small dark circles represent impact points of each leg with the ground. Whereas, small dark squares reveal states just after impact. Arrows are signs of behavior transition of each leg. The cycle of the passive gait consists of three steps in order that the compass robot returns to its initial state which is marked by solid squares. From an initial condition lying on the first cycle (marked by 1), the compass biped follows the cycles from 1 to 3 before it returns again to the first cycle.

Table II summarizes some characteristics of the period-three gait. It is clear that, from the first step (cycle) to the third step, the three quantities (namely the step length, the average velocity and the mechanical energy) of the biped robot increases. We showed in [3] that the increase in the average velocity and in the step length could have a fundamental rule for the control of the bipedal walking of the compass-gait biped robot to the period-three passive gait.

2) *Temporal Evolution:* Fig. 9 shows the temporal evolution of both angular positions and angular velocities of the two legs of the compass robot for $\varphi = 3.92$ deg. In fact, each leg can be either a stance leg or a swing leg. It is evident that the gait of the stance leg or the swing leg is of period-3. Actually, there is some kind of alternation between the left leg and the right one. Indeed, in spite of two successive steps are different, the left leg recaptures after three steps the same gait characteristic of the right leg. After exactly six steps,

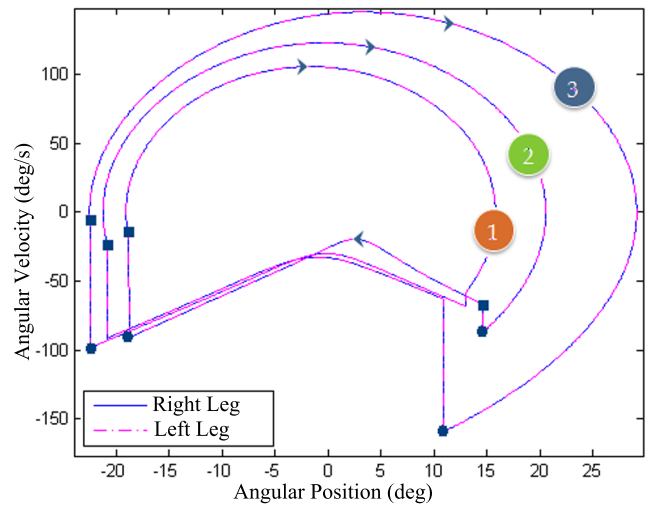


Fig. 8. A typical period-three passive limit cycle of the compass-gait biped for $\varphi = 3.92$ deg.

TABLE II. CHARACTERISTICS OF THE PERIOD-THREE PASSIVE GAIT.

Cycle number	Step length (m)	Average velocity (m/s)	Mechanical energy (J)
1	0.5125	0.6355	153.9906
2	0.5824	0.8982	154.3163
3	0.6350	0.8937	154.8982

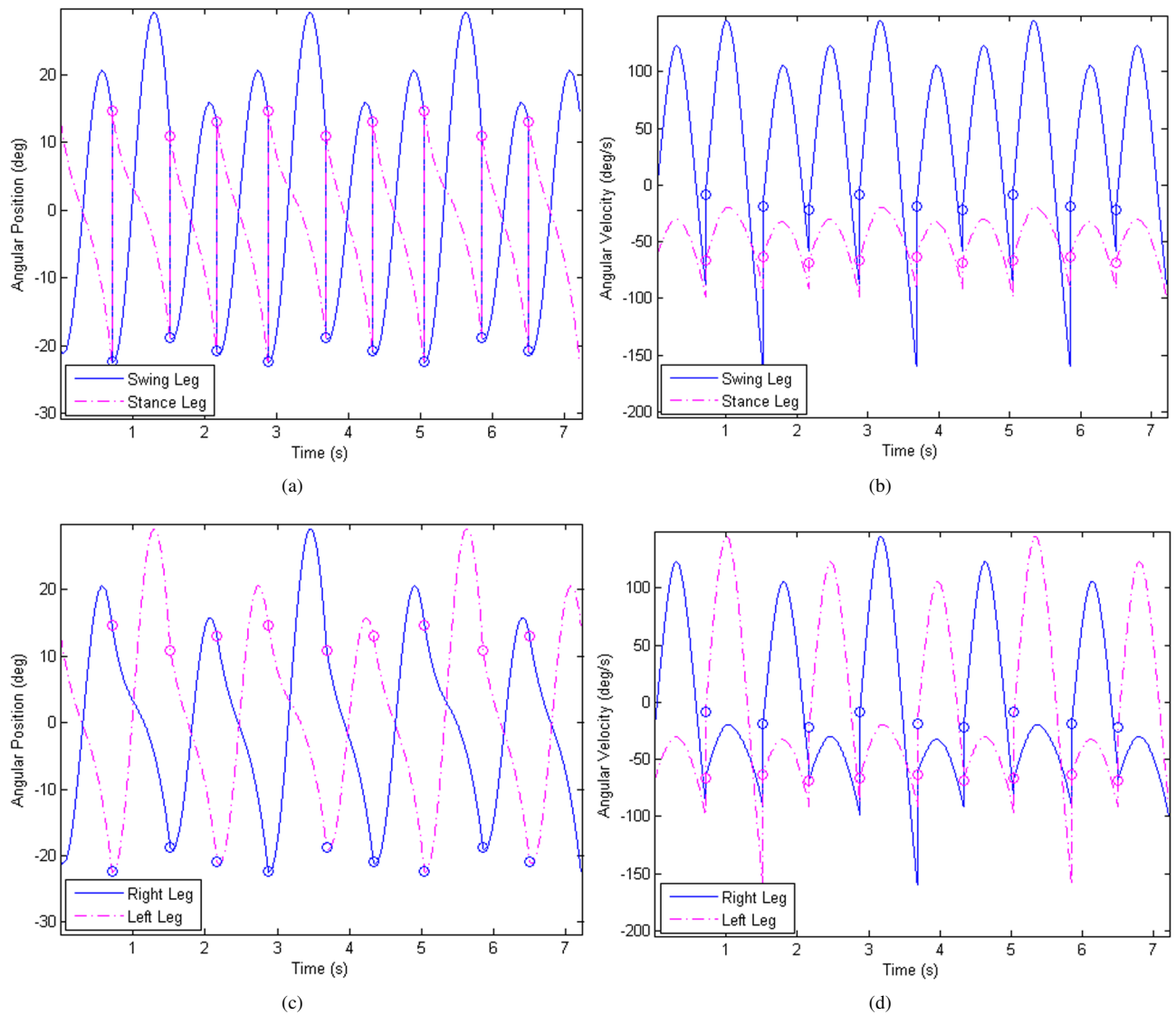


Fig. 9. Temporal evolution of the angular position (a and c) and the angular velocity (b and d) of the two legs of the compass biped for the period-three passive gait. In (a) and (b), continuous curve is for the swing leg whereas dashed curve is for the stance leg. In (c) and (d), continuous curve is for the right leg whereas dashed one is for the left leg.

the right leg picks up again its periodic gait. This alternation phenomenon between the two legs is very special and reveals some cooperation and coordination between the two legs of the compass robot in order to obtain a period-three stable periodic gait. Compared with the period-1 stable gait which is defined as symmetric and two consecutive steps are indistinguishable, the period-3 stable gait can have also some kind of symmetry. This symmetry is reached by coordination between the two legs of the compass robot to reach in consequence a successful typical stable passive walk.

3) *Energy Balance*: Fig. 10 shows variation of the kinetic energy of the compass-gait biped robot with respect to its potential energy during a walking cycle (which consists of three steps). This energy balance plot consists of constant potential energies (dashed lines) reflecting the impact on the ground, and parallel inclined lines indicating the swing phase. In addition, each energy path (line BC, or EF, or HI) is a straight line at an angle of 135 deg with the axis of the kinetic

energy. This confirms that the mechanical energy is evidently constant during each step. The trajectory of the compass-gait biped robot starts from the point A and follows the path ABCDEFGHI. Points C, F and I are the touchdown points of the swing leg with the ground. Horizontal lines CD, FG and IA the instantaneous loss of the kinetic energy produced by the impact with the walking surface. The mechanical energy of the compass-gait biped robot for the three steps is indicated in Table II. Obviously, the mechanical energies increases from the first step to the third one.

4) *Basin of Attraction of the Period-Three Gait*: The basin of attraction of the period-three gait and that of the period-one gait are shown in Fig. 11. The blue set is the basin of attraction of the period-one gait, whereas the pink set reveals the basin of attraction of the period-three gait. The remaining white set refers to the initial conditions from which the compass robot falls down. The basin of attraction of the period-one gait is depicted for the same slope angle $\varphi = 3.92$ deg. Each basin

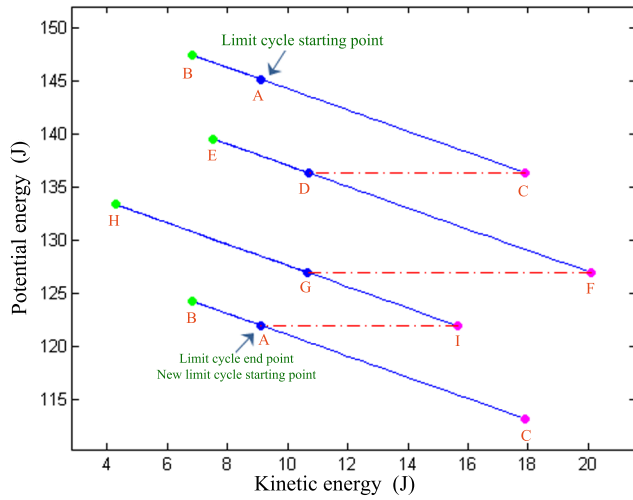


Fig. 10. Potential energy as a function of kinetic energy of the compass-gait biped robot for the period-three passive gait.

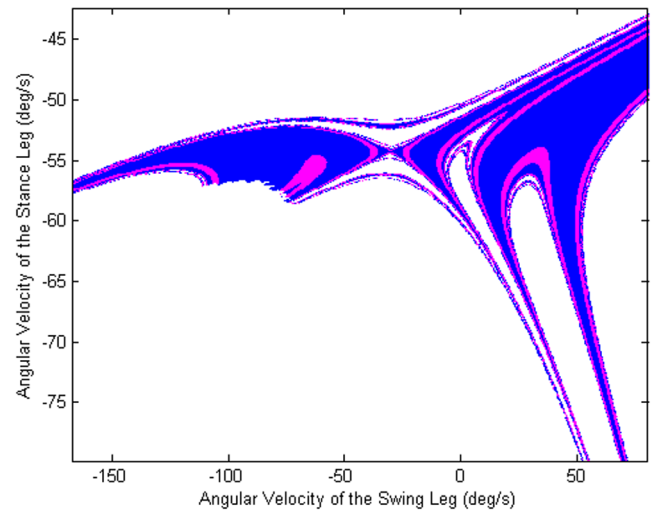
of attraction in Fig. 11 is plotted for a two state variables of the compass-gait model. Fig. 11a is depicted for a fixed initial position of the two legs of the compass biped robot. We have chosen $\theta_{ns} = -17$ deg and $\theta_s = -2\varphi - \theta_{ns}$, and we have varied the angular velocities of the two legs. However, Fig. 11b is plotted for a defined initial angular velocity of the compass robot: $\dot{\theta}_{ns} = 20$ deg/s and $\dot{\theta}_s = -50$ deg/s.

IV. CONCLUSIONS

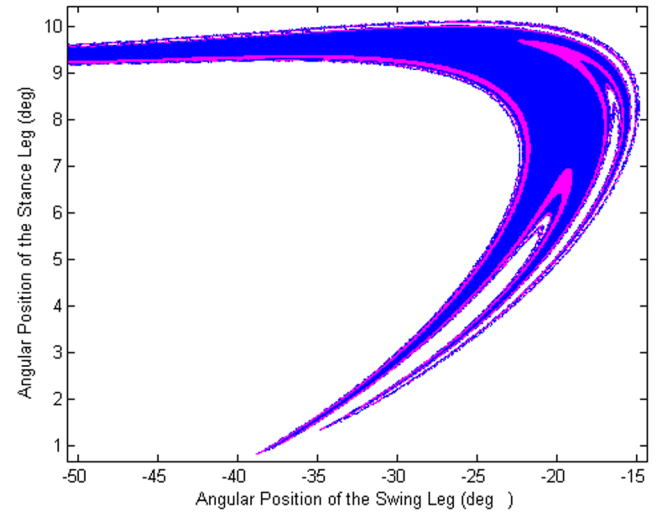
This work is a further study on passive dynamic walking of the compass-gait biped robot on steep slopes. We have investigated the period-three route to chaos generated in passive bipedal locomotion. We analyzed some characteristics of the period-three passive gait. This analysis was conducted with the state space, the time evolution, the energy balance and the basin of attraction. In addition, our investigation on order/chaos was carried out using the Lyapunov exponents and the fractal Lyapunov dimension. Different and attractive forms of the chaotic attractor have been illustrated. Its basin of attraction was also shown.

REFERENCES

- [1] A. Goswami, B. Thuilot and B. Espiau, Compass-like biped robot Part I: Stability and bifurcation of passive gaits, INRIA Technical Report, vol. 2996, 1996.
- [2] A. Goswami, B. Thuilot and B. Espiau, A study of the passive gait of a compass-like biped robot: Symmetry and chaos, *Int. J. of Robotics Research* vol. 17, 1998, pp. 1282–1301.
- [3] H. Gritli, N. Khraief and S. Belghith, A Period-Three Passive Gait Tracking Control for Bipedal Walking of a Compass-Gait Biped Robot, *the IEEE-2011 International Conference on Communications, Computing and Control Applications*, Hammamet, Tunisia (2011), pp. 01–06.
- [4] H. Gritli, N. Khraief and S. Belghith, Cyclic-fold bifurcation in passive bipedal walking of a compass-gait biped robot with leg length discrepancy, *Proc. IEEE International Conference on Mechatronics*, Istanbul, Turkey (2011), pp. 851–856.
- [5] H. Gritli, N. Khraief and S. Belghith, Falling of a Passive Compass-Gait Biped Robot Caused by a Boundary Crisis, *Pro. the 4th Chaotic Modeling and Simulation International Conference (CHAOS2011)*, Crete, Greece (2011), pp. 155–162.



(a)



(b)

Fig. 11. Basins of attraction of the period-one passive gait (blue) and the period-three passive gait (pink).

- [6] H. Gritli, S. Belghith and N. Khraief, Intermittency and interior crisis as route to chaos in dynamic walking of two biped robots, *International Journal of Bifurcation and Chaos*, vol. 22(3), 2012, Paper No. 1250056, 19 p.
- [7] H. Gritli, S. Belghith and N. Khraief, Cyclic-fold bifurcation and boundary crisis in dynamic walking of biped robots, *International Journal of Bifurcation and Chaos*, vol. 22(10), 2012, Paper No. 1250257, 15 p.
- [8] H. Gritli, N. Khraief and S. Belghith, Period-three route to chaos induced by a cyclic-fold bifurcation in passive dynamic walking of a compass-gait biped robot, *Communications in Nonlinear Science and Numerical Simulation*, vol. 17(11), 2012, pp 4356–4372.
- [9] H. Gritli, N. Khraief and S. Belghith, Chaos control in passive walking dynamics of a compass-gait model, *Communications in Nonlinear Science and Numerical Simulation*, vol. 18(8), 2013, pp. 2048–2065.
- [10] Q. Li and X. S. Yang, New walking dynamics in the simplest passive bipedal walking model, *Appl. Math. Model.*, vol. 36(11), 2012, pp. 5262–5271.
- [11] Q. Li, S. Tang and X-S. Yang, New bifurcations in the simplest passive walking model, *Chaos: An Interdisciplinary Journal of Nonlinear Science*, vol. 23, 2013, 043110 (14 pages).